Quantum Chemical and Kinetic Study of Formation of 2-Chlorophenoxy Radical from 2-Chlorophenol: Unimolecular Decomposition and Bimolecular Reactions with H, OH, Cl, and O_2

Mohammednoor Altarawneh, Bogdan Z. Dlugogorski,* Eric M. Kennedy, and John C. Mackie*,†

Process Safety and Environment Protection Research Group, School of Engineering, The University of Newcastle, Callaghan, NSW 2308, Australia

Received: December 31, 2007; In Final Form: February 3, 2008

This study investigates the kinetic parameters of the formation of the chlorophenoxy radical from the 2-chlorophenol molecule, a key precursor to polychlorinated dibenzo-*p*-dioxins and dibenzofurans (PCCD/F), in unimolecular and bimolecular reactions in the gas phase. The study develops the reaction potential energy surface for the unimolecular decomposition of 2-chlorophenol. The migration of the phenolic hydrogen to the *ortho*-C bearing the hydrogen atom produces 2-chlorocyclohexa-2,4-dienone through an activation barrier of 73.6 kcal/mol (0 K). This route holds more importance than the direct fission of Cl or the phenolic H. Reaction rate constants for the bimolecular reactions, 2-chlorophenol + X → X−H + 2-chlorophenoxy (X = H, OH, Cl, O_2) are calculated and compared with the available experimental kinetics for the analogous reactions of X with phenol. OH reaction with 2-chlorophenol produces 2-chlorophenoxy by direct abstraction rather than through addition and subsequent water elimination. The results of the present study will find applications in the construction of detailed kinetic models describing the formation of PCDD/F in the gas phase.

Introduction

Recent analyses of the formation mechanism of polychlorinated dibenzo-*p*-dioxins and polychlorinated dibenzofurans (PCDD/F) in the gas phase from chlorophenol precursors have shown that the pathways involving the self-coupling of chlorophenoxy radicals and the coupling of chlorophenoxy radicals with chlorophenol molecules are more important than the self-coupling of chlorophenol molecules.[1−5] Earlier kinetic models of the formation of PCDD/F assumed that the chlorinated phenoxy radicals react rapidly with molecular oxygen, making phenoxy radicals unavailable for the formation of PCDD/F.[6] However, owing to their significant resonance stabilization, considerable concentrations of chlorophenoxy radicals can build up in the combustion environment affording their self-condensation to PCDD/F congeners. Therefore, accurate modeling of PCDD/F formation demands the knowledge of the rate parameters for the formation of chlorophenoxy radicals from chlorophenols.

The present study employs 2-chlorophenol (2-C_6H_4ClOH) as a representative species of all polychlorophenols to model the formation of chlorophenoxy radicals. This selection of the chlorophenol molecule follows from the frequent use of 2-chlorophenol in studies on precursors for PCDD/F under oxidative and pyrolytic conditions.[7−9] Under pyrolytic conditions, the thermal decomposition induces the initial decay of a 2-chlorophenol molecule[9]

$$2\text{-}C_6H_4ClOH \rightarrow 2\text{-}C_6H_4ClO^{\bullet} + H \quad (1)$$

$$2\text{-}C_6H_4Cl(OH) \rightarrow [2\text{-}C_6H_4(OH)]^{\bullet} + Cl \quad (2)$$

Although several studies of the unimolecular decomposition of phenol itself exist, the present authors are unaware of a comparable study of chlorophenols. By kinetic modeling of a complex mechanism of the pyrolysis of phenol, Lovell et al.[10] have derived a rate constant of $k_{(1-\text{phenol})} = 2.67 \times 10^{16}$ exp(−44 700 K/*T*) s^{-1}, valid between 1070 and 1150 K, for the unimolecular scission of the H−O bond in phenol. A recent theoretical investigation has yielded a somewhat lower rate constant for the same reaction.[11] Direct expulsion of a Cl atom from chlorobenzene occurs with a rate constant of $k_{(2-\text{chlorobenzene})}$ (1070−1280 K) = 3.0×10^{15} exp(−48 100 K/*T*) s^{-1}, between 1070 and 1280 K,[12] which amounts to more than 2 orders of magnitude lower than the rate constant claimed previously for the H-fission of phenol. Thus, under pyrolytic conditions, it might be expected that the fission of the O−H bond constitutes the sole initiator of the decomposition of 2-chlorophenol.

In the presence of dioxygen, the decomposition of the 2-chlorophenol commences at lower temperatures.[7] Owing to the difference in bond strengths between the O and H in the hydroxyl group and C and H on the aromatic ring, a triplet oxygen molecule reacts initially with 2-chlorophenol by abstraction of its hydroxyl H

$$2\text{-}C_6H_4ClOH + O_2\ (^3\Sigma_g) \rightarrow 2\text{-}C_6H_4ClO^{\bullet} + HO_2 \quad (3)$$

Following the initiation, the consumption of 2-chlorophenol proceeds via the reactions involving H and OH radicals, formed from the decomposition of HO_2 radicals

* Corresponding author. E-mail: Bogdan.Dlugogorski@newcastle.edu.au; tel: (+61 2) 4921 6176; fax: (+61 2 4921 6920).
† Also at School of Chemistry, The University of Sydney.

10.1021/jp712168n CCC: $40.75
Published on Web 04/02/2008

$$HO_2 + M \rightarrow OH + H + M \quad (4)$$

$$2\text{-}C_6H_4ClOH + H \rightarrow 2\text{-}C_6H_4ClO^{\bullet} + H_2 \quad (5)$$

$$2\text{-}C_6H_4ClOH + OH \rightarrow 2\text{-}C_6H_4ClO^{\bullet} + H_2O \quad (6)$$

However, the presence of H and OH can also engender displacement reactions liberating Cl radicals. Pseudo-equilibrium calculations of Evans and Dellinger[8] have demonstrated that the concentration of Cl radicals exceeds that of OH over a wide range of temperatures.[8] According to the available rate constants for the reaction with phenol, Cl serves as the dominant abstractor of the phenolic H. Hence, one would expect an analogous reaction involving chlorophenol to correspond to

$$2\text{-}C_6H_4ClOH + Cl \rightarrow 2\text{-}C_6H_4ClO^{\bullet} + HCl \quad (7)$$

In the present study, we perform quantum chemical investigations using various density functional theory (DFT) methods to obtain reliable thermochemical and kinetics quantities for the above reactions of 2-chlorophenol. We also compare the results of our computations with the analogous rate data for phenol because none exist for 2-chlorophenol. Our new results will facilitate the construction of detailed kinetic models of the formation of PCDD/F in the gas phase.

Computational Details

It has been well established that the most popular hybrid density functional theory method of B3LYP[13,14] has a fundamental shortcoming in describing the potential energy surface (PES) around the transition states for hydrogen transfer reactions because of its inadequate characterization of the self-interaction correction.[15−18] To overcome this problem, the meta hybrid DFT method of BB1K[19] is used throughout this study, and its results are compared with those obtained using the B3LYP method. In addition to using an HF exchange fraction of 0.42 (compared with 0.20 in B3LYP), the BB1K method also abstracts kinetic energy density from Kohn−Sham orbitals by deploying the kinetic-energy-dependent dynamical correlation functional BB95.[20] Although the BB1K method is more effective in obtaining the barrier heights and geometries for the transition structures, the B3LYP method retains its success in extracting the reaction energies, vibrational frequencies, and structures for the molecules.[21] All structures have been optimized using the basis set of 6-31G(d).[22] Transition structures (TS) on potential energy surfaces have been characterized as first-order saddle points by possessing one and only one imaginary frequency. Transition structures were confirmed by connecting the related reactants and products by intrinsic reaction coordinate (IRC) analysis. Energies have been refined by performing single-point energy calculations using the extended basis set of 6-311G+(3df,2p). All optimizations have been executed using the Gaussian (G03) suite of programs.[23]

Internal rotations in the 2-chlorophenol molecule and some transition structures have been treated as hindered rotors, and their thermodynamic partition functions have replaced the partition functions of the corresponding harmonic oscillators. Such treatment is necessary for accurate calculation of rate constants.[24] Internal rotation barriers have been calculated by Gaussian carrying out relaxed scans at varying torsional angles. Reduced moments of inertia for these torsional modes have been calculated using a model of two unsymmetrical tops that rotate with respect to each other by the means of the MultiWell suite of programs.[25]

Rate constants, $k(T)$, for several reactions have been evaluated using

$$k(T) = \kappa(T) \times k_{TST}(T)$$

where

$$k_{TST}(T) = \frac{\sigma}{\beta h} \frac{q^{TS}(T)}{q^{A}(T)\, q^{B}(T)} e^{-\beta \Delta E_0^{TS}}$$

is the rate constant derived by the conventional transition state theory (TST),[26] σ is the reaction symmetry number, $\beta = (k_B T)^{-1}$, k_B is Boltzmann's constant, h is the Planck constant, $q^{TS}(T)$ is the thermodynamic partition function for the transition structure, $q^{A}(T)$ and $q^{B}(T)$ are the partition functions for the reactants, ΔE_0^{TS} is the classical barrier height, and $\kappa(T)$ is the transmission coefficient that accounts for the quantum tunneling corrections. Tunneling effects are accounted for using both the Wigner[27] and Eckart[28] methods. In the Wigner method, the transmission coefficient corresponds to

$$\kappa(T) = 1 + \frac{1}{24} (h\beta\omega^{TS})^2$$

where ω^{TS} denotes the imaginary frequency of the transition structure. According to the Eckart method, $\kappa(T)$ is estimated by using an approximate adiabatic ground-state potential curve based on the zero-curvature tunneling methodology (ZCT).[29]

Rate constants for certain reactions are calculated using canonical variational transition state theory (CVT)[30−32] where the reaction rate constant is minimized as a function of reaction coordinates (s) and temperature (T) by

$$k^{CVT}(T) = \min_s k^{GT}(T, s)$$

where $k^{GT}(T,s)$ signifies the rate constant from the generalized transition state theory. All of the proposed transition structures in CVT calculations retain one and only one imaginary frequency along the reaction pathway. Reaction rate constant calculations have been performed using the TheRate program.[33]

Results and Discussion

Unimolecular Decomposition of 2-Chlorophenol. Several decomposition channels have been investigated theoretically in order to describe a detailed mechanism for the pyrolysis of phenol[11,34]

$$C_6H_5OH \rightarrow C_5H_6 + CO \quad (8a)$$

$$\rightarrow C_6H_5O + H \quad (8b)$$

$$\rightarrow C_5H_4CO + H_2 \quad (8c)$$

$$\rightarrow C_6H_4 + H_2O \quad (8d)$$

Direct expulsion of H_2 or H_2O was shown not to be competitive with channel 8b (direct expulsion of the hydroxyl H atom) or 8a (the phenolic H transfer at the *ortho* carbon). The latter was shown[11] to provide the minimum energy pathway for the formation of the major experimental products of decomposition, CO and *cyclo*-C_5H_6.

In this section, we investigate the energetics and kinetics of the unimolecular formation of the 2-chlorophenoxy radical from 2-chlorophenol in the reactions analogous to those proposed for the decomposition of phenol.[11,34,35] Optimized geometries for

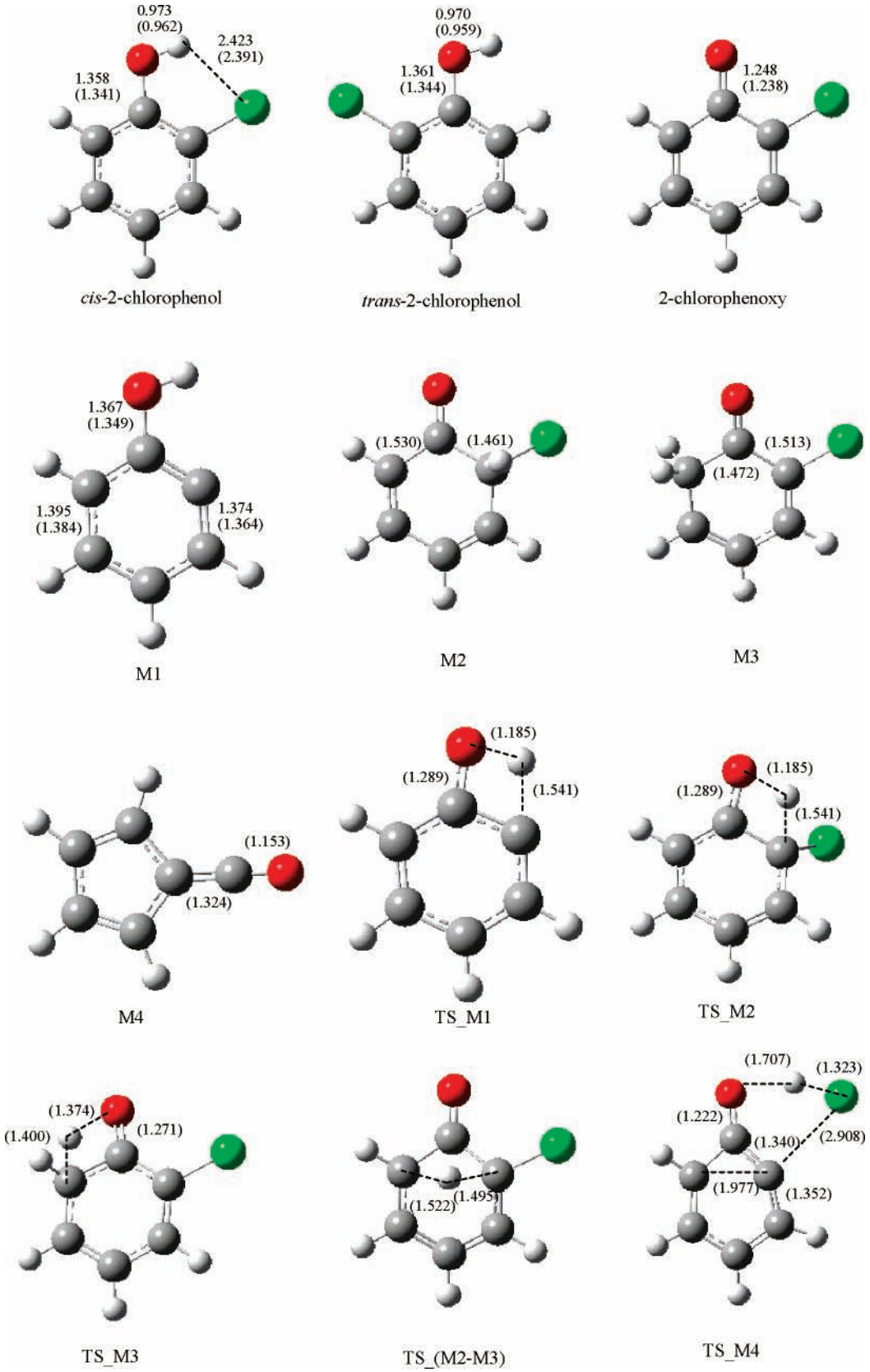

Figure 1. Optimized geometries for reactants, products, intermediates, and transition structures for the unimolecular decomposition of 2-chlorophenol calculated by BB1K (in brackets) and B3LYP methods using the basis set of 6-31G(d).

the reactants, products, intermediates, and transition structures for the unimolecular decomposition of 2-chlorophenol are shown in Figure 1; the reaction potential energy surface (PES) is displayed in Figure 2, with Table 1 listing the Arrhenius parameters for the high-pressure limit.

Direct H Expulsion from the Hydroxyl Group. Intramolecular hydrogen bonding in 2-chlorophenol produces two distinguishable conformational isomers, a trans form where the hydroxyl hydrogen points away from the chlorine atom and a cis form where the hydrogen is intramolecularly bonded to the chlorine

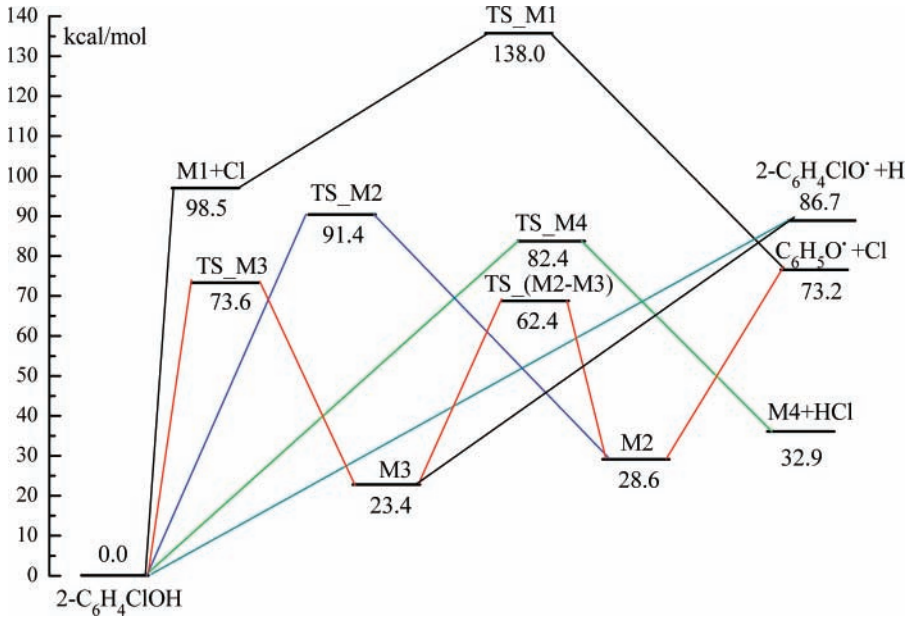

Figure 2. Schematic energy diagram predicted at the BB1K/6-311G+(3df,2p)//BB1K/6-31G(d) level of theory on the singlet-state potential energy surface for the unimolecular decomposition of 2-chlorophenol; for species identification, see Figure 1.

TABLE 1: Arrhenius Parameters for the Unimolecular Decomposition Reactions of 2-Chlorophenol and Its Bimolecular Reactions with H, OH, Cl, and O_2 ($^3\Sigma_g$), Fitted in the Temperature Region of 300−2000 K

reaction	A (s^{-1} or cm^3 $molecule^{-1}$ s^{-1})	n	E_a/R (K)	method
2-C_6H_4ClOH → M1 + Cl	1.03×10^{13}	0.453	43 000	B3LYP CVT
2-C_6H_4ClOH → M2	9.72×10^{9}	1.251	42 900	BB1K TST/Eckart
2-C_6H_4ClOH → M3	3.88×10^{11}	0.546	37 200	BB1K TST/Eckart
2-C_6H_4ClOH → M4 + HCl	8.27×10^{11}	0.958	42 000	BB1K TST/Eckart
2-C_6H_4ClOH → H + 2-$C_6H_4ClO^•$	1.84×10^{12}	0.69	44 000	BB1K CVT
2-C_6H_4ClOH + H → 2-$C_6H_4ClO^•$ + H_2	5.79×10^{-27}	4.781	1 620	BB1K TST/Eckart
2-C_6H_4ClOH + OH → 2-$C_6H_4ClO^•$ + H_2O	3.41×10^{-21}	2.681	1 070	BB1K TST/Eckart
2-C_6H_4ClOH + Cl → 2-$C_6H_4ClO^•$ + HCl	1.86×10^{-16}	1.468	−582	BB1K CVT
2-C_6H_4ClOH + O_2 ($^3\Sigma_g$) → 2-$C_6H_4ClO^•$ + HO_2	3.83×10^{-20}	2.432	13 200	B3LYP CVT

atom as shown in Figure 1. The presence of these two isomers has been confirmed experimentally from the differences in their hydroxyl group stretching frequencies. Both experimental[36,37] and theoretical[38] studies have found the presence of an intramolecular hydrogen bond in the cis form to make it more stable than its trans counterpart. Using the G3B3 ab initio method, the cis conformer was found to be more stable by 3.1 kcal/mol,[38] whereas experimentally, the difference in energy between the two isomers is no more than 1.7 kcal/mol.[36] Our value of 3.5 kcal/mol for the energy difference between the two isomers is in accord with previous theoretical estimations.[38] The difference between the theoretical and experimental estimations has been attributed to considerable overlapping between the OH vibrational bands in the two isomers that could not be unraveled adequately under the experimental conditions.[38] Transformation between these two isomers is computed using the BB1K method to involve a barrier of only 2.4 kcal/mol (0 K).

Table 2 lists the O−H bond energy in 2-chlorophenol obtained by calculating the energy for reaction 1 for both cis and trans conformers. The unimolecular O−H fission of *cis*-2-chlorophenol appears similarly endoergic as that of phenol where the bond energy equals 89.5 kcal/mol;[39] especially see the estimate from G3B3 in Table 2. Because the barrier to rotation of the hydroxyl group amounts to a trivial value under pyrolysis temperatures, an equilibrium population of *cis*- and *trans*-2-chlorophenol exists. In order to determine the reaction rate constant for H expulsion from *trans*-2-chlorophenol, we varied the O···H distance manually at intervals of 0.15 Å. Because the fission of O−H bond generates two free radicals, we performed the partial optimization using the singlet open shell BB1K with mixing of the frontier orbitals. We found that at separations of O···H of beyond 2.0 Å the energies of the transition structures gradually begin to exceed the energies of the separated reactants, presumably because of the system exhibiting multireference character (MRC). We have further

TABLE 2: Reaction Energy (kcal mol^{-1}) for the Direct H Expulsion from cis and trans Forms of 2-Chlorophenol (Reaction 1)

reaction	G3B3	BB1K	B3LYP
trans-2-chlorophenol → H + 2-chlorophenoxy	86.8	83.5	80.9
cis-2-chlorophenol → H + 2-chlorophenoxy	89.9	86.7	83.8

tested this case by using several different guesses for the initial wavefunction when deploying various theoretical methods, and in each case the transition state energy was found to be above that of the dissociation products beyond a separation of ~2.0 Å. To overcome this problem, we represented the energies at the minimum energy points (MEP) for the bond fission of O···H by the Morse function $V(r) = D_e\{1 - \exp -[\beta(r - r_e)]\}^2$ where r_e is the equilibrium O−H distance, r is O−H distance in the stretched structure, D_e is the electronic bond energy of OH and β equals $(k_e/2D_e)^{1/2}$ where k_e is the force constant for OH stretch. We have obtained $\beta = 2.61$ Å^{-1}, $r_e = 0.962$ Å, and $D_e = 95.3$ kcal/mol at the BB1K/6-311+G(3df,2p)//BB1K/6-31G(d) level. We computed the position of the transition structure (a point on the MEP) to be located at a separation of 2.40 Å. Finally, we fitted the high-pressure limit rate constant obtained for reaction 1 to the modified Arrhenius parameters in the temperature range of 600 to 2000 K to obtain

$$k_1 = 1.84 \times 10^{12}\, T^{0.69} \exp(-44\,000\ \mathrm{K}/T)\ \mathrm{s}^{-1}.$$

The experimental rate constant for phenol of Lovell et al.,[10] derived from the kinetic modeling and the analysis of end products, exceeds the calculated rate constant by almost 50 times. The experimental rate constant of Lovell et al. might possibly be overestimated owing to the presence of secondary reactions abstracting H, such as phenol + H, and cyclopentadienyl + phenol. Zhu and Bozzelli[35] have applied their thermochemical parameters, obtained from the quantum chemical calculations, together with the reverse reaction rate constant for phenoxy + H → phenol determined by He et al.,[40] to arrive at the rate constant for the forward reaction, phenol → phenoxy + H, as $7.63 \times 10^{14} \exp(-43\,700\ \mathrm{K}/T)\ \mathrm{s}^{-1}$. With our calculated values for the forward reaction and the thermochemical parameters of the reactants and the products, our computed rate constant for the reverse reaction (in 2-chlorophenol) lags behind their rate constant by a factor of about 5 at around 1000 K. Xu and Lin[11] determined theoretically a reaction rate constant for H expulsion from phenol to obtain $k_{(1-\mathrm{phenol})} = 3.33 \times 10^{17}\, T^{-0.51} \exp(-46\,100\ \mathrm{K}/T)\ \mathrm{s}^{-1}$, in the high-pressure limit and for temperatures between 800 and 2000 K. This reaction rate constant trails the experimental rate constant by 1 order of magnitude. We would not expect a significant modification of the phenol kinetics because of the chlorine atom in *trans*-2-chlorophenol; and from our detailed analysis for this reaction, their *A* factor must correspond to an extremely long O···H separation in the transition state (i.e., > ~3.5 Å). This interatomic distance seems rather large for a first-order saddle point involving H atom movement toward an O atom, and, according to our analysis, the resulting structure at such a distance cannot sustain a single imaginary frequency along the reaction coordinate.

It would therefore appear that the experimental rate constant for O−H fission in phenol[10] might be too high by a factor of at least 10 and does not accord with the reverse reaction rate constant of He et al.,[40] exceeding this latter value by an order of magnitude when calculated using the equilibrium constant. Furthermore, both the *A* factor and activation energy for the fission reaction as calculated by Xu and Lin[11] appear to be larger than that predicted by our thermochemistry, but the rate constant itself appears to be largely in accord with the reverse rate constant.[40]

Direct Cl Expulsion. The expulsion of the chlorine atom forms the 2-hydroxyphenyl radical (reaction 2). The fission of the C−Cl bond requires 92.5 and 98.5 kcal/mol (0 K) calculated from the B3LYP and BB1K methods, respectively. As shown in Figure 2, the migration of the phenolic hydrogen into the vacant ortho carbon affords the phenoxy radical. This reaction is exoergic by 25.3 kcal/mol with an activation barrier of 39.5 kcal/mol; see TS_M1 in Figure 1. The calculated strength of the C−Cl bond may be compared with a value of 97.0 kcal/mol for the same bond in chlorobenzene (C_6H_5Cl).[41]

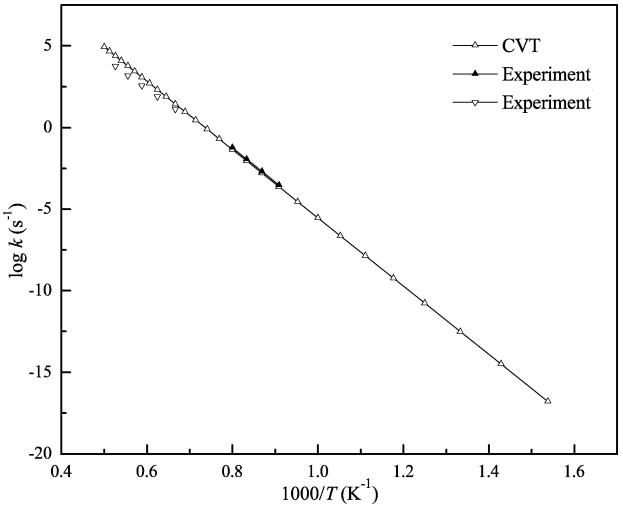

Figure 3. Comparison between the calculated rate constant for C−Cl fission in 2-chlorophenol using the B3LYP/6-311+G(3df,2p)//6-31G(d) level of theory and experimental high-pressure limit rate constants for fission of the C−Cl bond in chlorobenzene; (▲) ref 12; (▽) ref 42.

To describe the kinetics of the decomposition process, we constructed the minimum energy path for reaction 2 by varying manually the separation of C···Cl at an interval of 0.15 Å at the level of theory of BB1K/6-311+G(3df,2p)//BB1K/6-31G(d). Then, the rate constant for the direct fission of C−Cl followed from the CVT calculations. All of the input structures for CVT contained a single imaginary frequency corresponding to the stretching of the C···Cl bond. We calculated the high-pressure limit rate constant as a function of temperature and C···Cl bond length. We found that the reaction rate constant is the lowest for all temperatures when the C···Cl bond length corresponds to 3.410 Å, a distance that amounts to almost double the equilibrium bond length of C−Cl in 2-chlorophenol (1.768 Å). In fact, 3.410 Å constitutes the largest possible distance where the proposed input structure could retain a single imaginary vibrational frequency along the reaction coordinate. As shown in Figure 3, the calculated rate constant agrees very well with the experimental values of the rate constant for the unimolecular decomposition of chlorobenzene into phenyl and chlorine atoms.[12,42] The high-pressure limit rate constant obtained by CVT for reaction 2, fitted to the modified Arrhenius parameters in the temperature range of 600 to 2000 K, results in

$$k_2 = 1.03 \times 10^{13}\, T^{0.453} \exp(-43\,000\ \mathrm{K}/T)\ \mathrm{s}^{-1}.$$

Phenolic H Migration to the Ortho Carbons. As illustrated in Figure 2, the hydrogen transfer to the ortho carbon atoms bearing correspondingly the chlorine and hydrogen atoms affords the products M2 and M3 (6-chlorocyclohexa-2,4-dienone and 2-chlorocyclohexa-2,4-dienone). These are located 28.6 and 23.4 kcal/mol above 2-chlorophenol, respectively. An energy barrier of 91.4 kcal/mol (TS_M2) accompanies the formation of M2 from 2-chlorophenol, higher by 17.8 kcal/mol than the energy of activation required for the formation of M3 (TS-M3). Hydrogen transfer between the two ortho carbons takes place via the transition structure TS_(M2−M3), 33.8 kcal/mol above

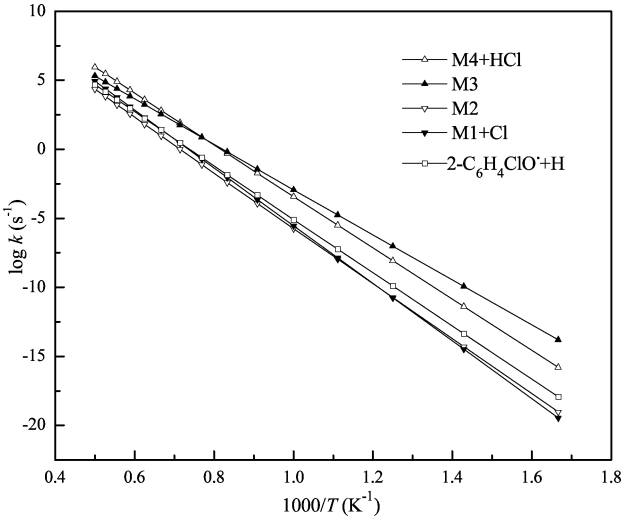

Figure 4. Arrhenius plot for the reaction rate constants in the high-pressure limit for the unimolecular decomposition of 2-chlorophenol into various reaction channels calculated at the BB1K/6-311+G(3df,-2p)//BB1K/6-31G(d) level of theory.

M2. M2 can eliminate the out-of-plane Cl to produce the non-chlorinated phenoxy without intrinsic barrier; similarly M3 can eliminate H from C6 to produce 2-chlorophenoxy and a H atom. Finally, M4 can be formed through a direct elimination of HCl in a concerted process via the transition structure TS_M4 affording the closed-shell structure of M4, which requires surmounting a sizable barrier of 82.4 kcal/mol. However, this barrier is about 20 kcal/mol lower than the barrier calculated previously for direct H_2 elimination from phenol.[11,43]

We have applied the conventional transition state theory (TST) to calculate the rate constants in the high-pressure limit, as reported in Figure 4 and Table 1S in the Supporting Information. Tunneling effects for all reactions appear negligible over the studied temperature range. The reaction $C_6H_4ClOH \rightarrow$ M3 dominates other channels up to 1100 K. At temperatures higher than 1100 K, direct elimination of HCl to form M4 becomes competitive with the formation of M3. This finding agrees with the importance of 2,4-cyclohexadienone (the non-chlorinated M3) as the major initial intermediate in phenol pyrolysis.[43,44]

The unimolecular formation of 2-chlorophenoxy from M3 has been investigated by performing a MultiWell analysis[25] for the reactions (H + 2-chlorophenoxy $\rightarrow$ M3 $\rightarrow$ 2-chlorophenol). We find this reaction process to be significantly pressure-dependent between 10 and 0.1 atm and between 500 and 1600 K. At 1 atm and above and at a temperature of 1000 K, most of the reaction flux proceeds to 2-chlorophenol. At 1000 K, the rate of the formation of 2-chlorophenol equates to 1.1×10^{-12} cm^3 molecule^{-1} s^{-1}, slower by more than 2 orders of magnitude than the formation of 2-chlorophenol via the direct H recombination with 2-chlorophenoxy, the latter characterized by the experimental rate constant of 3.3×10^{-10} cm^3 molecule^{-1} s^{-1}.[40] Thus, the formation of 2-chlorophenoxy from M3 constitutes only a minor channel for its formation compared with the direct H expulsion from the hydroxyl group. The most likely exit channel for M3 leads the formation of *cyclo*-C_5H_5Cl and CO, analogously with the proposed pyrolysis mechanism for phenol.[11]

Bimolecular Reaction of 2-Chlorophenol with H. We have used this reaction as a case to compare between phenol systems and chlorophenol systems as well as to study the effect of the position and the number of chlorine atoms on reaction and activation energies. Table 3 reports the reaction and activation energies for the direct abstraction of H from the hydroxyl group of phenol and various chlorophenol congeners by the H radical. The barrier heights ($\Delta E_0^{\ddagger}$) for the abstraction process from phenol, 2-chlorophenol, 3-chlorophenol, and 4-chlorophenol obtained by the BB1K method amount to 10.3, 13.1, 10.8, and 9.8 kcal/mol, respectively. It has been shown that an introduction of a chlorine atom in the phenol molecule does have a slight effect on the molecular properties of the chlorophenol in comparison with the phenol molecule.[43,44] The most prominent source of this effect arises from intermolecular hydrogen bonding between the hydroxyl hydrogen and the chlorine atom. The intermolecular hydrogen bonding is most evident in the 2-chlorophenol molecule (ortho) and is much weaker in the 3-chlorophenol (meta) and the 4-chlorophenol (para) molecules. For example, the harmonic vibrational frequency of the stretch in the hydroxyl group υ(O−H) in the 2-chlorophenol molecule was calculated to be reduced by 90 cm^{-1} with respect to the phenol molecule, whereas the υ(O−H) value in 3-chlorophenol and 4-chlorophenol, where hydrogen bonding is absent, is the same as that for the phenol molecule. Because of the intermolecular hydrogen bonding, the barrier height for the phenolic H abstraction by the H radical in the 2-chlorophenol molecule is calculated to be 2.8 kcal/mol higher than the corresponding value for the phenol molecule, whereas the barriers for 3-chlorophenol and 4-chlorophenol are very close to the corresponding value in the phenol molecule.

TABLE 3: Reaction and Activation Energies for the Abstraction of Phenolic Hydrogen by H Atom from Phenol and Various Chlorinated Phenols (Reaction 5)

method	reactant	ΔE	$\Delta E_0^{\ddagger}$
BB1K	phenol	−16.0	10.3
	2-chlorophenol	−14.1	13.1
	3-chlorophenol	−14.9	10.8
	4-chlorophenol	−17.2	9.8
	2,5-dichlorophenol	−13.2	13.1
	2,3,5-trichlorophenol	−13.0	13.4
	pentachlorophenol	−14.8	12.6
B3LYP	phenol	−21.5	3.5
	2-chlorophenol	−21.4	5.4

Another source for the effect of the chlorine atom on the phenol ring with respect to the phenol molecule comes from the interaction between the hydroxyl group and the chlorine atom through the phenol ring.[43] As an electron-withdrawing group, the chlorine atom pulls the electron density from the negatively charged hydroxyl group through the phenol ring. When introducing multiple chlorine atoms to the phenol ring, the electron density captured from the hydroxyl group as well as the phenolic ring is shared between the chlorine atoms. As a result, the calculated barrier heights for the abstraction process from other ortho substituents, that is, 2,5-dichlorophenol (13.1 kcal/mol), 2,3,5-trichlorophenol (13.4 kcal/mol), and pentachlorophenol (12.6 kcal/mol), are close to the calculated value for the abstraction process from the 2-chlorophenol molecule (13.1 kcal/mol). Generally, it has been shown that molecular properties of multiply chlorinated phenols are systematically changed with the number and position of chlorine atoms; for example, bond distances in the 19 chlorophenol congeners have been measured to be different by 0.001−0.006 Å from the parent phenol's counterparts,[43] while the hydroxyl bond energies have been calculated to vary by 2.0−3.3 kcal/mol with respect to the phenol molecule.[45] In a nutshell, we have shown that the 2-chlorophenol molecule could be effectively used to model all chlorinated congeners of phenol, especially ortho substituents,

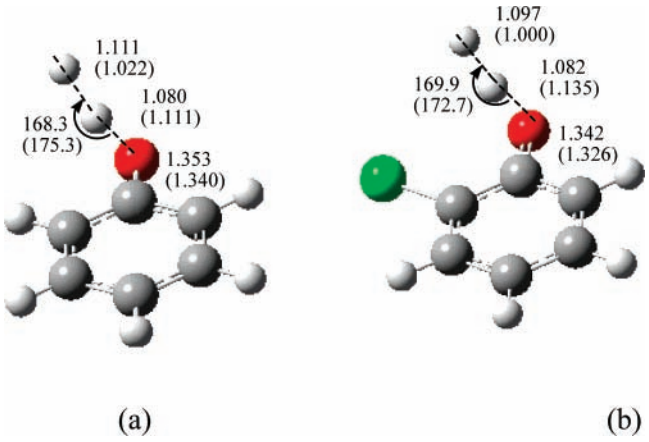

Figure 5. Transition structures optimized by the B3LYP and BB1K (in brackets) methods with the 6-31G(d) basis set for the abstraction of phenolic oxygen by H atom from (a) phenol and (b) 2-chlorophenol.

which are more relevant to the formation of PCDD/Fs than para and meta substituents.[1]

The BB1K barrier height for the reaction with phenol leads to an experimental activation energy of 12.5 kcal/mol, obtained from the fitted Arrhenius formula of the reaction rate constant as a function of temperature. Figure 5 illustrates the transition structures for the H abstraction reactions for phenol and 2-chlorophenol. The slight difference in geometries displayed in this figure for the transition structures for reactions with phenol and 2-chlorophenol expresses the effect caused by ortho chlorine discussed above. According to the BB1K method, the interatomic distance of H−O in the TS for 2-chlorophenol elongates by 18% from the equilibrium position of 0.962 Å. The reaction energy ($\Delta E_0^{\ddagger}$, 0 K) corresponds to −14.1 and −21.4 kcal/mol, using BB1K and B3LYP, respectively, compared with a value of −25.0 kcal/mol reported previously, obtained by means of the semiempirical molecular orbital method of AM1.[8]

Rate Constant Calculations. In this section, we report the rate constant for phenolic H abstraction from 2-chlorophenol and compare its numerical value with available experimental measurements for phenol. Internal rotor barriers have been calculated for the rotation of the hydroxyl group in 2-chlorophenol about the O−C bond and for the rotation of H−H group around the O−C bond in the transition structure; as displayed in Figure 5. Figures 1S and 2S in the Supporting Information depict the rotor potential energy for 2-chlorophenol and the transition structure, respectively. The potential energy profile for the internal rotor in the transition structure has been constructed as a function of the dihedral angle by scanning the torsional angles from 0° to 360° at an interval of 30°, while keeping frozen the distances corresponding to forming or breaking bonds (H···H and H···O) and allowing the remaining structural parameters to relax. We have calculated the barriers for the internal rotation in 2-chlorophenol to be 6.7 and 7.0 kcal/mol, by means of the BB1K/6-31G(d) and B3LYP/6-31G(d) methods, respectively. The internal rotor potential displayed in Figure 1S exhibits a minimum corresponding to the *trans*-2-chlorophenol form, necessitating its treatment as a hindered rotor, rather than a harmonic oscillator, in the ensuing analysis.

We employed various theoretical approaches to calculate the rate constant of reaction 5. These include the use of conventional transition state theory (TST) with tunneling effect based on the Wigner method (W) and Miller's one-dimensional Eckart tunneling model using energetics and canonical variational transition state theory (CVT) with small curvature tunneling

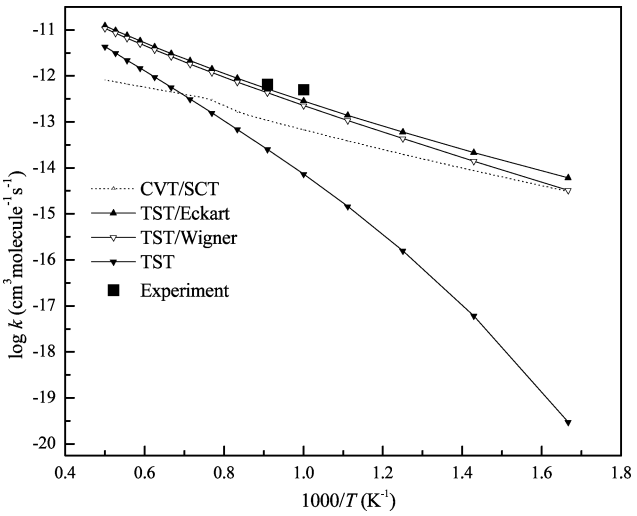

Figure 6. Arrhenius plot for the reaction rate constant for $C_6H_4ClOH + H \rightarrow C_6H_4ClO^{\bullet} + H_2$ calculated at the BB1K/6-311+G(3df,2p)//BB1K/6-31G(d) level of theory; (■) ref 40.

(SCT). The calculated reaction rate constants are shown in Figure 6 and Table 2S along with the available experimental data for the non-chlorinated phenol.

Significant values of imaginary frequencies ($\omega^{\ddagger}$) of 2265.4*i* and 1551.8*i* calculated, respectively, by means of BB1K and B3LYP methods, characterize the transition vector for the abstraction process. Thus quantum tunneling is expected to increase the calculated rate constants considerably, especially at low temperatures. The calculated transmission coefficient $\kappa(T)$ at 600 K evaluates to 3.82 from the Eckart method, decreasing to 1.75 and 1.25 at 1000 and 2000 K, respectively. Reaction rate constants obtained from the BB1K method with TST/Eck and TST/W corrections differ from the available experimental measurements for phenol by factors of 1.2 and 2.9, respectively. The following equation describes the rate constant with Eckart correction fitted to an Arrhenius expression

$$k_5 = 5.8 \times 10^{-27}\, T^{4.779} \exp(-1620\ \mathrm{K}/T)\ \mathrm{cm^3\ molecule^{-1}\ s^{-1}}$$

Treating the internal rotations as harmonic oscillators, rather than hindered rotors, reduces the calculated rate constant almost by a factor of 3. The reaction rate constants obtained from B3LYP-based calculations overestimate the BB1K-derived rate constants as well as the experimental values by about 1 order of magnitude.

For the CVT/SCT calculation of rate constants for reaction 5, the minimum energy points (MEP) of the potential energy surface have been obtained at the BB1K/6-311+G(3df,2p)//BB1K/6-31G(d) level of theory in the mass-weighted Cartesian coordinates (*s*) with a step of 0.05 amu$^{1/2}$ b, according to the Gonzalez−Schlegel steepest descent path. We have calculated the vibrational frequencies at 12 selected points (6 points on the reactants side and 6 points on the products side from −0.3−0.3 amu$^{1/2}$ b) to generate the required energetic information for the potential energy surface. Figure 7 depicts the classical energy barriers (V_c), the vibrational zero point energies (ZPE), and the vibrational ground-state adiabatic barriers (V_g^a) along the MEP potential. The CVT/SCT reaction rate constant, fitted to the modified Arrhenius expression, yields

$$k_5 = 6.0 \times 10^{-10}\, T^{-0.387} \exp(-6290\ \mathrm{K}/T)\ \mathrm{cm^3\ molecule^{-1}\ s^{-1}}$$

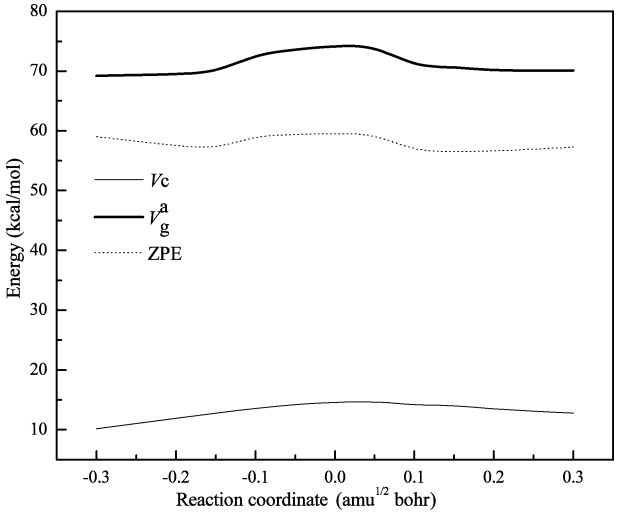

Figure 7. Potential energy surface for the reaction $C_6H_4Cl(OH) + H \rightarrow 2\text{-}C_6H_4ClO^{\bullet} + H_2$ calculated at the BB1K/6-311+G(3df,2p)//BB1K/6-31G(d) level of theory in the vicinity of the transition structure. V_c is the classical adiabatic ground state potential curve, V_g^a is the vibrationally adiabatic ground state potential curve, and ZPE is the total vibrational zero point energy.

At 1000 K, the CVT/SCT underestimates the (phenol) experimental value by a factor of 5.5. The *k*(TST/Eck)/*k*(CVT/SCT) ratios correspond to 2.0, 4.4, 6.9, and 15 at 600, 1000, 1500, and 2000 K, respectively. These values indicate that the variational effect for this reaction becomes prominent as temperature increases.

Bimolecular Reaction of 2-Chlorophenol with OH. Experimental studies have been performed for the reaction between the OH radical and phenol in aqueous media[48−51] as well as in gaseous environment,[40,51−54] usually under atmospheric conditions, where OH reaction with phenol proceeds through fast addition to the ring to form a π adduct, rather than through abstraction to form water. This initial π adduct either dissociates back into OH and phenol or dioxygen adds to the radical sites of the adduct. For phenol, OH addition takes place preferentially at the ortho (48%) and the para (36%) positions to produce dihydroxy−cyclohexadienyl radicals. ipso addition could not be distinguished from direct H abstraction to give phenol, and both have been postulated to contribute around 8% of the total reaction rate at room temperature.[55] At high temperatures, direct abstraction of the phenolic hydrogen becomes the dominant channel.[54]

Direct Abstraction. Lundqvist and Eriksson[54] postulated a direct abstraction of the phenolic hydrogen by the hydroxyl radical, without a transition structure.[56] However, we have located a transition state for the direct abstraction for *cis*- and *trans*-2-chlorophenol as shown in Figure 8, using both B3LYP and BB1K methods. Though, the transition structures calculated by means of B3LYP exhibit negative barriers. In TS_OH(*cis*) computed at the BB1K/6-31G(d) level of theory, the phenolic O−H bond elongates by 10% from the equilibrium intermolecular distance of 0.962 Å and the abstraction takes place nearly linearly, as shown by the geometry of TS_OH(*cis*) in Figure 8.

Concerning the more stable cis conformer, we have found that the OH radical forms three prereactive complexes (PR) in the vicinity of the phenolic hydroxyl group. Figure 8 displays the structures of these prereactive complexes. PR1 and PR2 occur for geometries intermediate between the transition state for the direct abstraction process and the separated reactants (OH and 2-chlorophenol), falling 2.5 and 2.0 kcal/mol below the separated reactants (BB1K/6-311+G(3df,2p)//BB1K/6-31G(d)), respectively. We note that Xu and Lin[11] had discovered prereactive complexes between OH and phenol previously. PR1 contains one very small vibrational imaginary frequency (23*i* cm^{-1}) corresponding to the motion of the hydroxyl group toward the chlorine atom. The vibrational frequency υ_3 (145 cm^{-1}) reflects the reaction coordinate of the abstraction process. PR2 contains no imaginary frequency, and the vibrational frequency υ_4 (144 cm^{-1}) signifies the reaction coordinate.

Reaction 6 takes place in two steps, the first involving the formation of the prereactive complexes PR1 and PR2, and the second occurring via the abstraction of phenolic H leading to the formation of the 2-chlorophenoxy radical and a water molecule.

$$2\text{-}C_6H_4Cl(OH) + OH \leftrightarrow \begin{matrix}PR1\\PR2\end{matrix} \quad (6a)$$

$$\begin{matrix}PR1\\PR2\end{matrix} \xleftrightarrow{TS\_OH(cis)} 2\text{-}C_6H_4Cl(O^{\bullet}) + H_2O \quad (6b)$$

Considering the non-chlorinated phenol as a benchmark for comparison, the barrier height calculated for reaction 6 (without considering the very shallow PR1/PR2) corresponds to 3.0 kcal/mol, slightly higher than the experimental value of 2.6 kcal/mol.[54] The reaction energy for reaction 6 using BB1K and B3LYP amounts to −27.1 and −33.7 kcal/mol, respectively.

OH Addition to the Ring. We have considered OH addition to the ortho carbon atoms bearing hydrogen and chlorine as well as ipso addition to the carbon bearing the hydroxyl group. Figure 9 displays the corresponding transition structures, and the energetics are given in Table 4. We were unable to find optimized prereactive complexes for the addition reactions at the two ortho positions or the ipso additions despite significant efforts using BB1K and B3LYP methods. All initial structures were eventually optimized to one of the PR1-3 structures shown previously in Figure 8. The presence of two pairs of lone electrons on the oxygen atom of the hydroxyl group enables the formation of an intramolecular bond with the phenolic hydrogen, which may hinder the formation of a direct prereactive complex for OH addition in the vicinity of the hydroxyl group (the two ortho sites). This postulate is supported by us locating a genuine prereactive complex for OH addition on the para carbon, distant from the phenolic hydroxyl. In the transition structures for OH addition, the hydroxyl group approaches perpendicular to the ring where the oxygen atom points downward toward the ring at a distance of ∼2.100 and 1.980 Å using B3LYP and BB1K methods, respectively, and the hydrogen, the chlorine, and the hydroxyl group at each corresponding addition site distort slightly backward to accommodate the approaching OH radical.

We have obtained negative energy barriers of 1.6 kcal/mol for the addition reaction using the B3LYP functional, in accord with findings of other researchers investigating aromatic compounds with the same method.[57−60] Employing the BB1K functional, we have calculated the energy barriers of 2.3, 3.1, and 4.5 kcal/mol, respectively, for OH addition to the ortho carbon bearing the hydrogen atom, the carbon bearing the hydroxyl group, and the ortho carbon bearing the chlorine atom. As we aim to investigate thermodynamics and kinetics of the chlorophenoxy formation, detailed studies of addition reactions, which do not lead to the formation of chlorophenoxy radical, fall beyond the scope of this article. In brief, the addition of OH at the ortho carbon bearing the chlorine atom eliminates the chlorine atom in one step affording catechol and a chlorine atom, without the formation of a π adduct as a first step. The addition of OH at the ortho carbon bearing the hydrogen atom

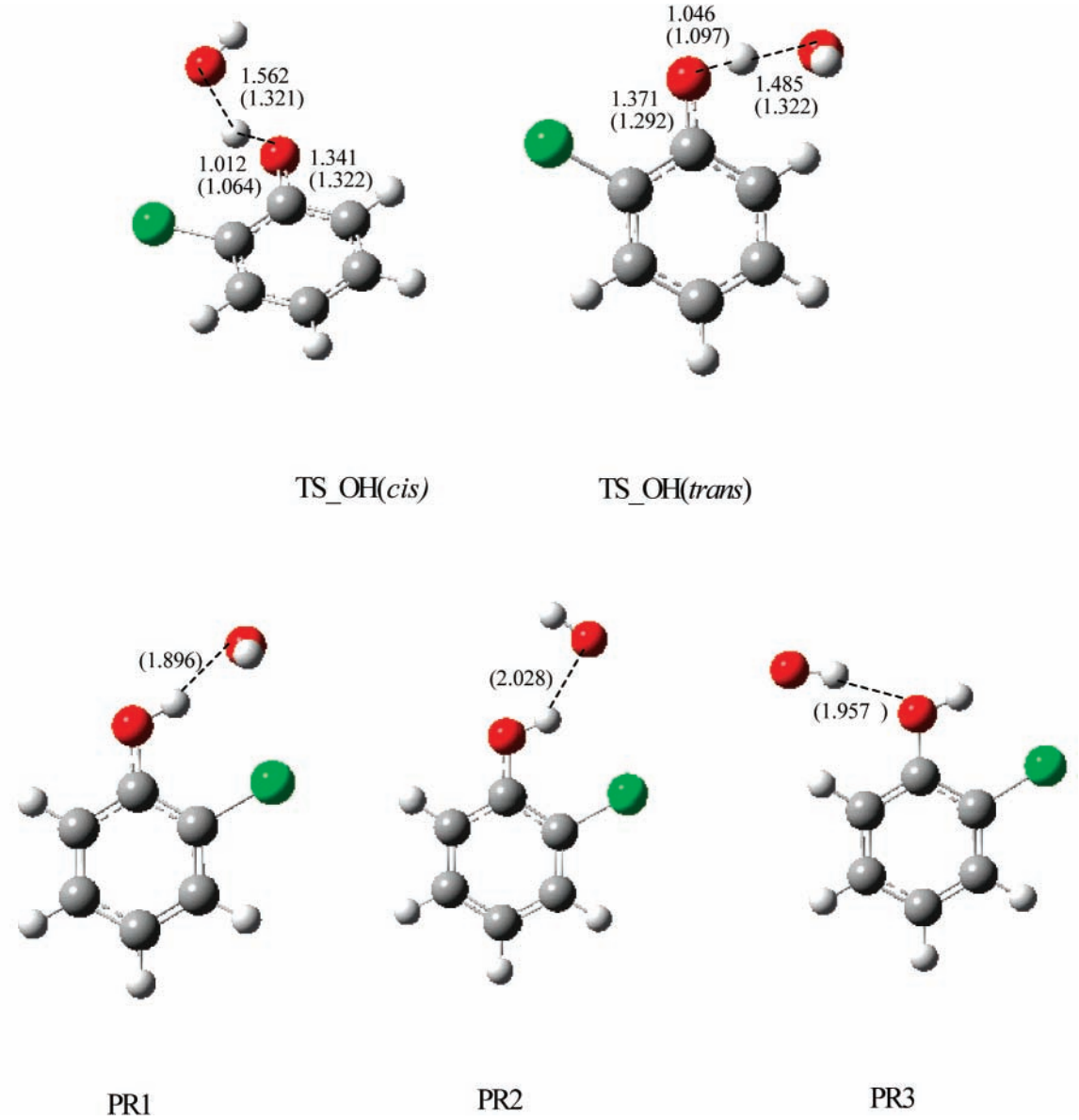

Figure 8. Transition structures and prereactive complexes for the abstraction of phenolic oxygen from 2-chlorophenol by the hydroxyl group, optimized by means of the B3LYP and BB1K (in brackets) methods using the basis set of 6-31G(d).

yields the π adduct of 2-$C_6H_4Cl(OH)_2$ trapped in a potential well of 18.6 kcal/mol in depth with respect to the separated reactants.

Direct elimination of water to produce phenoxy from the analogous non-chlorinated adduct has been investigated theoretically[56] and experimentally.[49,54] According to these studies, water elimination requires an activation energy of 19.1 kcal/mol (PMP2 method).[56] This compares with our finding, from the BB1K method, of a barrier for the removal of water of 26.2 kcal/mol with respect to the adduct 2-$C_6H_4Cl(OH)_2$ and 9.2 kcal/mol with respect to the separated reactants. We have located no similar transition structures for water elimination from the *ipso*-2-$C_6H_4Cl(OH)_2$ adduct.

Rate Constant Calculations. We report reaction rate constants for the two channels of 2-chlorophenol consumption by OH

$$2\text{-}C_6H_4ClOH + OH \rightarrow 2\text{-}C_6H_4ClO^{\bullet} + H_2O \qquad (6)$$

$$2\text{-}C_6H_4ClOH + OH \rightarrow 2\text{-}C_6H_4Cl(OH)_2 \qquad (6c)$$

As for calculation of the rate constant for reaction 5, we treat the internal rotations in all species and transition structures as hindered rotors and correct the partition functions accordingly. The potential energy profile for the internal rotor in the transition structure has been built as a function of the dihedral angle by scanning the torsional angles, while allowing all structural parameters to relax, except for the distances corresponding to forming or breaking bonds (H···O(hydroxyl) and H···O(phenolic)). On the basis of the computational results involving the BB1K functional with the Eckart tunneling correction TST/Eck, the rate constant for reaction 6 fitted to the modified Arrhenius relation leads to

$$k_6 = 3.4 \times 10^{-21}\, T^{2.681} \exp(-1070\ \mathrm{K}/T)\ \mathrm{cm^3\ molecule^{-1}\ s^{-1}}$$

Figure 10 and Table 3S provide the reaction rate constants, together with a comparison with available, but limited, experimental measurement for an analogues reaction of phenol with OH.

The reported experimental values of the reaction rate constants for phenol at low[54] (T = 300 K) and high[40] ($T \sim$ 1000 K)

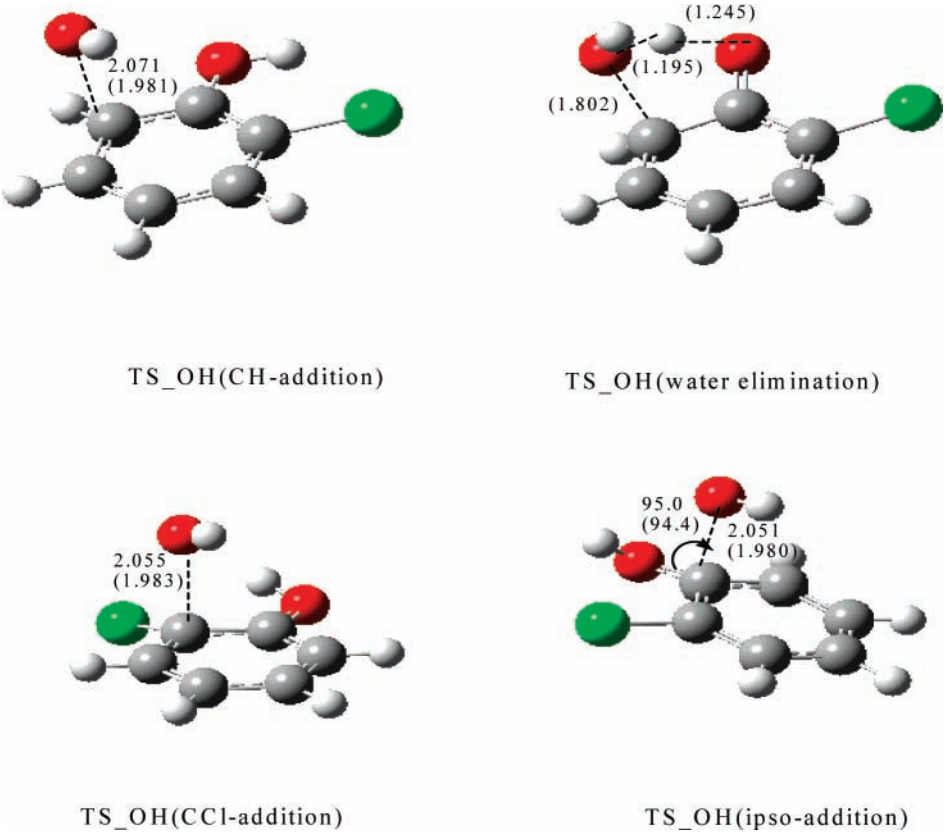

Figure 9. Transition structures for the addition of the OH radical to the 2-chlorophenol molecule and the subsequent elimination of water, optimized using the B3LYP and BB1K (in brackets) methods with the basis set of 6-31G(d).

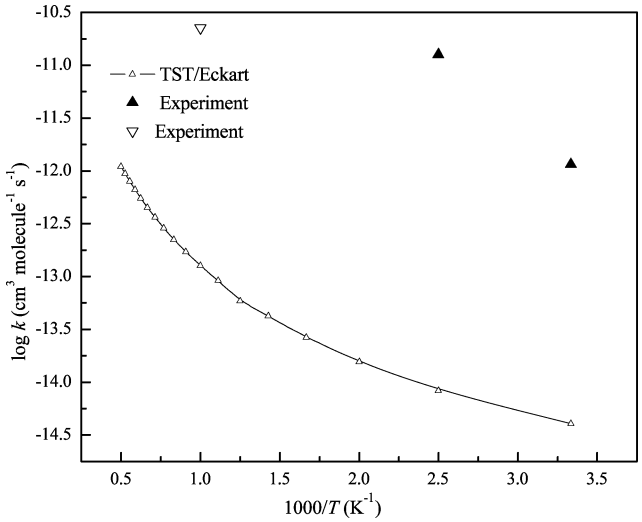

Figure 10. Arrhenius plots for the reaction rate constant for $C_6H_4ClOH + OH \rightarrow C_6H_4ClO^{\bullet} + H_2O$ calculated at the BB1K/6-311+G(3df,2p)//BB1K/6-31G(d) level of theory; (▲) ref 54; (▽) ref 40.

temperatures exceed those obtained from our calculations almost by a factor of 50. He et al.[40] reported a value for k_6 at the single temperature of 1032 K. In their study, they measured the rate constant for the reaction $H + C_6H_5OH \rightarrow H_2 + C_6H_5O$ by a comparative rate technique in which the decomposition of hexamethylethane to *t*-butyl radicals and then to isobutene engendered H atoms. He et al. compared the rate of the $H + C_6H_5OH$ reactions (to $H_2 + C_6H_5O$ and to $C_6H_6 + OH$) with the known rate of $H + CH_4 \rightarrow H_2 + CH_3$. To study the rate of $OH + C_6H_5OH$, these researchers replaced the methane with CO to remove the displaced OH radicals via $OH + CO \rightarrow CO_2 + H$ and measured the consequent increase in the concentration of C_6H_6. However, very large quantities of CO were needed to produce only slight increases in benzene concentrations. As a consequence, He et al. have concluded that their value for the phenolic H abstraction by OH could include a significant error owing to the great difference in the reactivity between phenol and the CO reference material with respect to the reaction with OH.

TABLE 4: Energetics of the Reactions Involving the Hydroxyl Group (OH) and the 2-Chlorophenol Molecule

reaction		ΔE	$\Delta E_0^{\ddagger}$
$2\text{-}C_6H_4Cl(OH) + OH \rightarrow 2\text{-}C_6H_4ClO^{\bullet} + H_2O$	BB1K	−27.1	3.0
	B3LYP	−33.7	−6.4
$2\text{-}C_6H_4Cl(OH) + OH \rightarrow 2\text{-}C_6H_4Cl(OH)_2$	BB1K	−16.7	2.3
	B3LYP	−15.8	−1.6
$2\text{-}C_6H_4Cl(OH)_2 \rightarrow 2\text{-}C_6H_4ClO^{\bullet} + H_2O$	BB1K	−10.1	26.2
	B3LYP	−15.0	17.3
$2\text{-}C_6H_4ClOH + OH \rightarrow$ *ipso*-$2\text{-}C_6H_4Cl(OH)_2$	BB1K	3.1	−17.0
	B3LYP	−0.1	−18.7

Knispel et al.[54] performed a low-temperature study (300−400 K) to determine the reaction rate for the abstraction channel by measuring the exponential decay of OH radicals, presumably because of their direct phenolic H abstraction. The authors did not measure the reaction products. Exponential decay of OH could not be limited to its consumption via the abstraction channel but could also involve the formation of prereactive complexes, such as PR1 and PR2 which should be stable at around 300 K. This may explain the very large difference between the calculated and experimental values at low temperature for reaction 6.

The calculated BB1K rate constant for the addition channel (at the ortho carbon bearing hydrogen) at 298 K amounts to

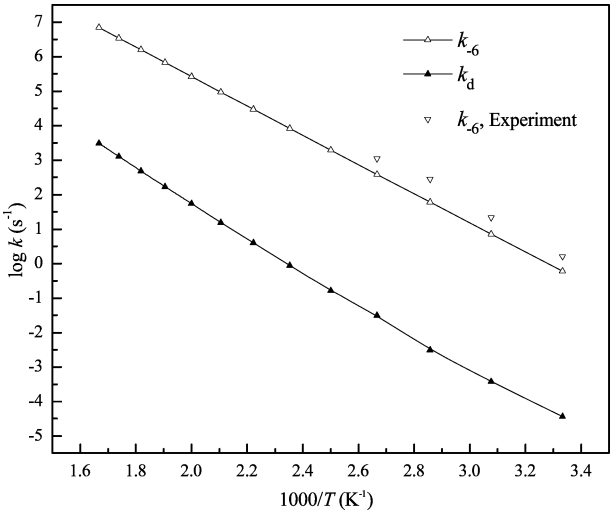

Figure 11. Rate constants in the high-pressure limit for the unimolecular decomposition of 2-$C_6H_4Cl(OH)_2$; (▽) ref 54.

6.65×10^{-15} cm^3 $molecule^{-1}$ s^{-1}, in contrast to the well-established rate constants for OH addition to the aromatics including benzene and phenol, which lie in the range of 1 to 50 $\times 10^{-12}$ cm^3 $molecule^{-1}$ s^{-1}.[52,54] The BB1K barrier for OH addition at this site is 2.3 kcal/mol compared to an experimentally determined negative activation energy for phenol of −1.3 kcal/mol.[54] Incidentally, we note our B3LYP barrier of −1.6 kcal/mol. These findings reminisce those of Chen and Bozzelli,[57] who have investigated the addition reaction of OH to benzene and have obtained positive barriers from G3 and negative barriers for DFT methods for the addition process. In particular, the G3 barriers required downward adjustment of 1.2 kcal/mol to match the experimental measurements.

In view of the large discrepancy between our computed results and available experimental measurements for reaction channels 6 and 6c, it is inappropriate to calculate the branching ratio for these two channels with respect to temperature. Nevertheless, we can report computed kinetic parameters for the exit channels of the chemically activated 2-$C_6H_4Cl(OH)_2$ adduct produced from OH + 2-C_6H_4ClOH.

It is well established that OH addition to aromatics to form a π adduct predominates over the direct abstraction channel for temperatures as high as 450 K. In atmospheric studies, formation of this adduct initiates the decomposition of an aromatic via oxygen addition and subsequent decomposition reactions. In the case of phenol, this adduct either eliminates water to form the phenoxy radical or dissociates back to the hydroxyl radical and phenol

$$2\text{-}C_6H_4ClOH + OH \xleftarrow{k_{-6c}} 2\text{-}C_6H_4Cl(OH)_2 \xrightarrow{k_{6d}} 2\text{-}C_6H_4ClO^{\bullet} + H_2O$$

High-pressure limit rate constants for k_{-6c} and k_{6d} have been calculated and fitted to modified Arrhenius parameters in the temperature range of 300−600 K and presented in Figure 11 and Table 4S. Dissociation back to the initial reactants proceeds rapidly compared with the rate of formation of 2-chlorophenoxy radical via water elimination at all temperatures, in accord with the observed rapid reversibility for OH-addition reactions of aromatics including phenol and benzene in the gas phase.[61] As depicted in Figure 11 and Table 4S, our results for k_{-6c} (dissociation of OH from the adduct) agree well with the experimental values of Knispel et al.[54] Thus, chlorophenoxy formation through reaction with OH takes place predominantly by direct abstraction, rather than through addition to the ortho position of the ring and subsequent elimination of water, even at low temperatures.

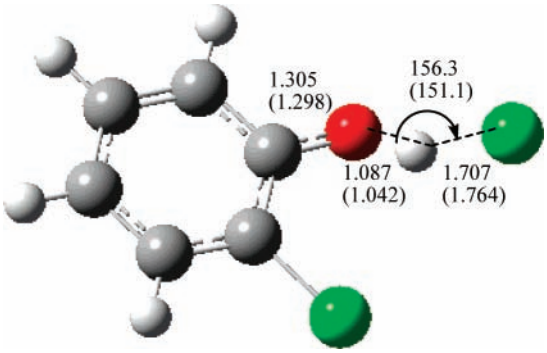

Figure 12. Transition structure for the reaction $C_6H_4ClOH + Cl \rightarrow C_6H_4ClO^{\bullet} + HCl$ optimized at the B3LYP and BB1K (in brackets) methods using the basis set of 6-31G(d).

Bimolecular Reaction with Cl. Gaseous Cl plays a major role in the formation of PCDD/F. Cl atom concentration can contribute up to 18% of the total chlorine content in the combustion environment of chlorinated hydrocarbons.[62] Oxidizing radicals (O and OH) promote the formation of Cl from the most abundant chlorine species, HCl, in a series of exothermic reactions.[8] Significant populations of Cl atoms exist in practical combustion systems, such as incineration of chlorinated wastes.

In this section, we study the formation of chlorophenoxy radical via reaction of chlorophenol with a Cl radical. We locate a transition structure for the direct abstraction of the phenolic H by Cl radical by a means of B3LYP and BB1K methods (Figure 12). The transition structure lies 2.3 and 10.5 kcal/mol below the separated reactants, respectively, from BB1K and B3LYP, whereas the reaction exoergicity corresponds, in that order, to 15.2 and 20.2 kcal/mol. To calculate the reaction rate constant, we generate the MEP curve employing the same procedure as that for calculating the CVT rate constant for abstraction of phenolic hydrogen by the hydrogen radical. Fitting of the CVT to the modified Arrhenius expression yields

$$k_7 = 1.9 \times 10^{-16}\, T^{1.645} \exp(582\ \text{K}/T)\ \text{cm}^3\ \text{molecule}^{-1}\ \text{s}^{-1}$$

To the best of our knowledge, the only experimental value for this rate constant has been reported by Platz et al.,[63] at 296 K. Our value at this temperature lags the experimental measurement by 1 order of magnitude. It should be noted that around 300 K the (experimental) rate constant for hydrogen abstraction by chlorine exceeds 125 times the H abstraction by OH.

Bimolecular Reaction with O_2. The decomposition of 2-chlorophenol in the presence of oxygen commences at around 873 K, a temperature 150 K lower than the observed onset temperature for decomposition of 2-chlorophenol under purely pyrolytic conditions.[7] Because the addition of triplet oxygen O_2 ($^3\Sigma_g$) to the 2-chlorophenol moiety is spin-forbidden, 2-chlorophenol consumption by O_2 has been attributed to phenolic H abstraction to form HO_2 and the 2-chlorophenoxy radical (reaction 3). No experimental rate constant for reaction 3 exists even for phenol itself. In a kinetic model for phenol oxidation, Brezinsky et al.[43] have estimated the rate constant for this reaction by substituting the corresponding value for H abstraction from the methyl group in toluene by oxygen molecule because the benzyl-H bond energy in toluene (87.5 kcal/mol)[64] is approximately the same as the O−H bond energy in phenol.

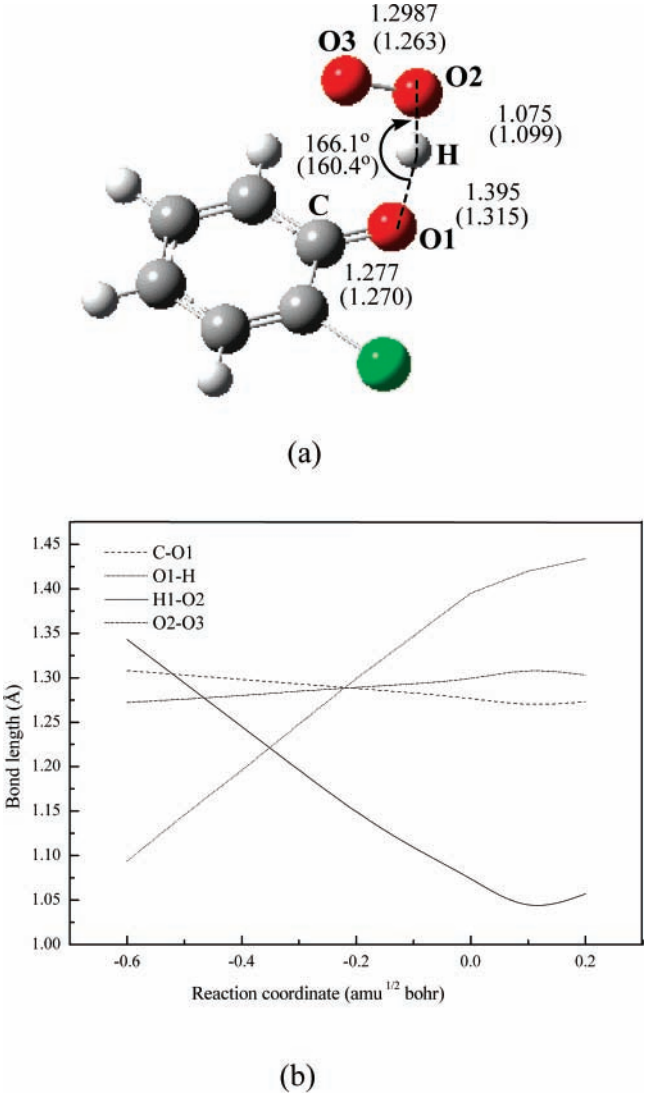

Figure 13. (a) Geometry of the transition structure for the reaction 2-$C_6H_4ClOH + O_2$ ($^3\Sigma_g$) → 2-$C_6H_4ClO^\bullet + HO_2$ optimized using B3LYP and BB1K (in brackets) with the basis set of 6-31G(d). (b) Bond length changes along the reaction coordinates using the B3LYP method with a single-point energy calculated with the 6-311+G(3df,2p) basis set.

Figure 13a shows the transition structure for triplet oxygen abstracting the phenolic H. Calculations using BB1K and B3LYP methods estimate the location of this transition structure to lie, respectively, 33.3 and 27.2 kcal/mol above the separated reactants, that is, oxygen and 2-chlorophenol. These values fall below the energy of the reaction products (2-chlorophenoxy and HO_2) by 7.3 and 9.2 kcal/mol, as computed from BB1K and B3LYP methods, respectively. This indicates a barrierless reaction, with the reactants transformed into the products without passing over an intrinsic energy barrier. Such behavior is expected because several theoretical studies have determined the transition structures for oxygen abstracting hydrogen from alkanes and other molecules to be located below the products.[65−67] We have also observed similar behavior for the abstraction of H from benzene by O_2. In order to derive the rate constant for the reaction, we have generated the MEP pathway from the relaxed structures along the reaction coordinate centered by the transition structure, finding that only the structures in the region of −0.5−0.2 amu$^{1/2}$ b retained a single imaginary frequency along the reaction coordinate. Because of this consideration, these structures have been used as candidate transition configurations for the CVT rate constant calculations. Figure 13 plots

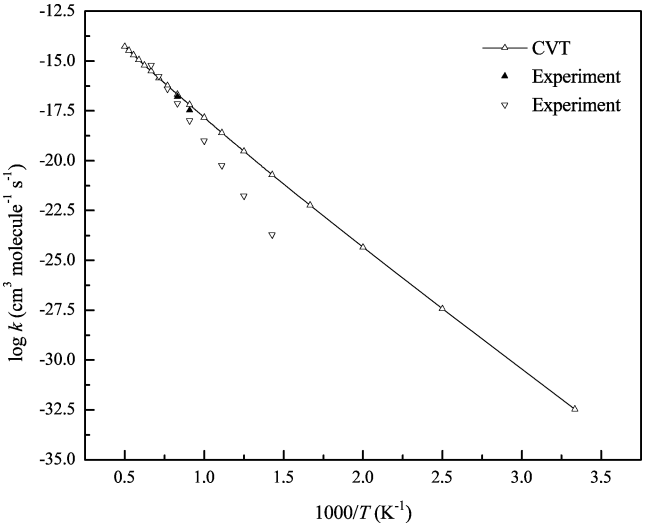

Figure 14. Arrhenius plots for the rate constant for the reaction 2-$C_6H_4ClOH + O_2$ ($^3\Sigma_g$) → 2-$C_6H_4ClO^\bullet + HO_2$ calculated at the B3LYP/6311+G(3df,2p)//B3LYP/6-31G(d) level of theory along with the experimentally determined rate constants for the related reaction of $C_6H_5CH_3 \rightarrow C_6H_5CH_2^\bullet + HO_2$; (▲) ref 68; (▽) ref 69.

the changes in the most important bond lengths in relaxed structures along the MEP pathway. We have fitted the CVT rate constant to the modified Arrhenius expression and have obtained

$$k_3 = 3.8 \times 10^{-20}\, T^{2.432} \exp(-13200\ \mathrm{K}/T)\ \mathrm{cm}^3\ \mathrm{molecule}^{-1}\ \mathrm{s}^{-1}$$

In Figure 14, we compare the calculated rate constant with the rate constant of the analogous reaction, $C_6H_5CH_3 + O_2 \rightarrow C_6H_5CH_2 + HO_2$, where the energy requirements are quite similar.[68,69] The CVT rate constant agrees reasonably well with the experimental rate constant for this analogous reaction, especially at elevated temperatures.

Conclusions

This contribution reports the reaction rate constants for the unimolecular decomposition of 2-chlorophenol as well as for its bimolecular reactions with H, OH, Cl radicals, and O_2 ($^3\Sigma_g$). Reactants, products, and transition structures have been optimized with the DFT method of B3LYP and also with the more recently developed meta hybrid DFT functional BB1K; the latter has been shown to give more accurate energy barriers. Reaction rate constants have been computed using conventional transition state theory (TST) with corrections for the quantum tunneling effects and by using the canonical variational transition state theory (CVT) for barrierless reactions. The low-frequency vibrational modes present in the transition structures for the phenolic H abstraction by H and OH radicals have been omitted from the rigid rotor harmonic oscillator and treated as hindered rotors. Rate constants for phenolic H abstraction by H, Cl, and O_2 accord with the experimental values for the analogous reactions involving phenol (for H and Cl) and toluene (for O_2). Large discrepancies between theoretical and sparse experimental data for the reaction between OH and (chloro-)phenols have been observed and warrant further studies. Results from the present investigation should provide useful data on the kinetics of conversion of the 2-chlorophenol molecule into the 2-chlorophenoxy radical, a core component in detailed kinetic models for the formation of PCDD/F in the gas phase.

Acknowledgment. This study has been funded by the Australian Research Council and supported by a grant of computing time from the Australian Centre of Advanced Computing and Communications (ac^3). M.A. acknowledges the award of a postgraduate studentship by the Al-Hussein Bin Talal University (Jordan).

Supporting Information Available: Calculated total energies, zero point energies, Cartesian coordinates, moments of inertia, and vibrational frequencies of all equilibrium and transition state structures. This material is available free of charge via the Internet at http://pubs.acs.org.

References and Notes

(1) Altarawneh, M.; Dlugogorski, B. Z.; Kennedy, E. M.; Mackie, J. C. *J. Phys. Chem. A* **2007**, *111*, 2563.
(2) Wiater, I.; Born, J. G. P.; Louw, R. *Eur. J. Org. Chem.* **2000**, *2000*, 921.
(3) Khachatryan, L.; Asatryan, R.; Dellinger, B. *Chemosphere* **2003**, *52*, 695.
(4) Altwicker, E. R.; Milligan, M. S. *Chemosphere* **1993**, *27*, 301.
(5) Altwicker, E. R. *Chemosphere* **1996**, *33*, 1897.
(6) Shaub, W. M.; Tsang, W. *Environ. Sci. Technol.* **1983**, *17*, 721.
(7) Evans, C. S.; Dellinger, B. *Environ. Sci. Technol.* **2005**, *39*, 122.
(8) Evans, C. S.; Dellinger, B. *Environ. Sci. Technol.* **2006**, *40*, 3036.
(9) Evans, C. S.; Dellinger, B. *Environ. Sci. Technol.* **2003**, *37*, 1325.
(10) Lovell, A. B.; Brezinsky, K.; Glassman, I. *Int. J. Chem. Kinet.* **1989**, *21*, 547.
(11) Xu, Z. F.; Lin, M. C. *J. Phys. Chem. A* **2006**, *110*, 1672.
(12) Ritter, E. R.; Bozzelli, J. W.; Dean, A. M. *J. Phys. Chem.* **1990**, *94*, 2493.
(13) Becke, A. D. *J. Chem. Phys.* **1993**, *98*, 5648.
(14) Lee, C.; Yang, W.; Parr, R. G. *Phys. Rev. B.* **1988**, *37*, 785.
(15) Lynch, B. J.; Truhlar, D. G. *J. Phys. Chem. A* **2001**, *105*, 2936.
(16) Polo, V.; Kraka, E.; Cremer, D. *Theor. Chem Acc.* **2002**, *107*, 291.
(17) Durant, J. L. *Chem. Phys. Lett.* **1996**, *256*, 595.
(18) Eriksson, L. A.; Kryachko, E. S.; Nguyen, M. T. *Int. J. Quantum Chem.* **2004**, *99*, 841.
(19) Zhao, Y.; Lynch, B. J.; Truhlar, D. G. *J. Phys. Chem. A* **2004**, *108*, 2715.
(20) Becke, A. D. *J. Chem. Phys.* **1996**, *104*, 1040.
(21) Zhao, Y.; Gonzalez-Garcia, N.; Truhlar, D. G. *J. Phys. Chem. A* **2005**, *109*, 2012.
(22) Montgomery, J. A.; Ochterski, J. W.; Petersson, G. A. *J. Chem. Phys.* **1994**, *101*, 5900.
(23) Frisch, M. J.; Trucks, G. W.; Schlegel, H. B.; Scuseria, G. E.; Robb, M. A.; Cheeseman, J. R.; Montgomery, J. A., Jr.; Vreven, T.; Kudin, K. N.; Burant, J. C.; Millam, J. M.; Iyengar, S. S.; Tomasi, J.; Barone, V.; Mennucci, B.; Cossi, M.; Scalmani, G.; Rega, N.; Petersson, G. A.; Nakatsuji, H.; Hada, M.; Ehara, M.; Toyota, K.; Fukuda, R.; Hasegawa, J.; Ishida, M.; Nakajima, T.; Honda, Y.; Kitao, O.; Nakai, H.; Klene, M.; Li, X.; Knox, J. E.; Hratchian, H. P.; Cross, J. B.; Bakken, V.; Adamo, C.; Jaramillo, J.; Gomperts, R.; Stratmann, R. E.; Yazyev, O.; Austin, A. J.; Cammi, R.; Pomelli, C.; Ochterski, J. W.; Ayala, P. Y.; Morokuma, K.; Voth, G. A.; Salvador, P.; Dannenberg, J. J.; Zakrzewski, V. G.; Dapprich, S.; Daniels, A. D.; Strain, M. C.; Farkas, O.; Malick, D. K.; Rabuck, A. D.; Raghavachari, K.; Foresman, J. B.; Ortiz, J. V.; Cui, Q.; Baboul, A. G.; Clifford, S.; Cioslowski, J.; Stefanov, B. B.; Liu, G.; Liashenko, A.; Piskorz, P.; Komaromi, I.; Martin, R. L.; Fox, D. J.; Keith, T.; Al-Laham, M. A.; Peng, C. Y.; Nanayakkara, A.; Challacombe, M.; Gill, P. M. W.; Johnson, B.; Chen, W.; Wong, M. W.; Gonzalez, C.; Pople, J. A. *Gaussian 03*, revision C.02; Gaussian, Inc.: Wallingford, CT, 2004.
(24) Vansteenkiste, P.; Neck, D. V.; Speybroeck, V. V.; Waroquier, M. *J. Chem. Phys.* **2006**, *124*, 044314.
(25) Barker, J. R. *Int. J. Chem. Kinet.* **2001**, *33*, 232.
(26) Eyring, H. *J. Chem. Phys.* **1935**, *3*, 107.
(27) Wigner, E. *J. Chem. Phys.* **1937**, *5*, 720.
(28) Eckart, C. *Phys. Rev.* **1930**, *35*, 1303.
(29) Marcus, R. A.; Coltrin, M. E. *J. Chem. Phys.* **1977**, *67*, 2609.
(30) Truhlar, D. G.; Isaacson, A. D.; Garrett, B. C. Generalized Transition State Theory. In *Theory of Chemical Reaction Dynamics*; Baer, M., Ed.; CRC Press: Boca Raton, FL, 1985; Vol. 4, p 65.
(31) Fast, P. L.; Truhlar, D. G. *J. Chem. Phys.* **1998**, *109*, 3721.
(32) Garrett, B. C.; Truhlar, D. G. *J. Chem. Phys.* **1979**, *70*, 1593.
(33) Duncan, W. T.; Bell, R. L.; Truong, T. N. *J. Comput. Chem.* **1998**, *19*, 1039.
(34) Le, H. T.; Flammang, R.; Gerbaux, P.; Bouchoux, G.; Nguyen, M. T. *J. Phys. Chem. A* **2001**, *105*, 11582.
(35) Zhu, L.; Bozzelli, J. W. *J. Phys. Chem. A* **2003**, *107*, 3696.
(36) Carlson, G. L.; Fateley, W. G.; Manocha, A. S.; Bentley, F. F. *J. Phys. Chem.* **1972**, *76*, 1553.
(37) Omi, T.; Shitomi, H.; Sekiya, N.; Takazawa, K.; Fujii, M. *Chem. Phys. Lett.* **1996**, *252*, 287.
(38) Shin, D. N.; Hahn, J. W.; Jung, K.; Ha, T. *J. Raman. Spectrosc.* **1998**, *29*, 245.
(39) da Silva, G.; Chen, C.-C.; Bozzelli, J. W. *Chem. Phys. Lett.* **2006**, *424*, 42.
(40) He, Y. Z.; Mallard, W. G.; Tsang, W. *J. Phys. Chem.* **1988**, *92*, 2196.
(41) Afeefy, H. Y.; Liebman, J. F.; Stein, S. E. Neutral Thermochemical Data. In *NIST Chemistry WebBook, NIST Standard Reference Database*; Linstrom, P. J., Mallard, W. G., Ed.; National Institute of Standards and Technology: Gaithersburg, MD, 2005; http://webbook.nist.gov., 2005; Vol. 69.
(42) Rao, V. S.; Skinner, G. B. *J. Phys. Chem.* **1988**, *92*, 2442.
(43) Brezinsky, K.; Pecullan, M.; Glassman, I. *J. Phys. Chem. A* **1998**, *102*, 8614.
(44) Manion, J. A.; Louw, R. *J. Phys. Chem.* **1989**, *93*, 3563.
(45) Han, J.; Deming, R. L.; Tao, F.-M. *J. Phys. Chem. A* **2004**, *108*, 7736.
(46) Koll, A.; Parasuk, V.; Parasuk, W.; Karpfen, A.; Wolschann, P. *J. Mol. Struct: THEOCHEM* **2004**, *700*, 81.
(47) Sanots, R. M. B.; Simoes, J. A. M. *J. Phys. Chem. Ref. Data* **1998**, *27*, 707.
(48) Mvula, E.; Schuchmann, M. N.; Sonntag, C. *J. Chem. Soc., Perkin Trans.* **2001**, *2*, 264.
(49) Bonin, J.; Janik, I.; Janik, D.; Bartels, D. M. *J. Phys. Chem. A* **2007**, *111*, 1869.
(50) Bansal, K. M.; Henglein, A. *J. Phys. Chem.* **1974**, *78*, 160.
(51) Brendt, T.; Boge, O. *Phys. Chem. Chem. Phys.* **2003**, *5*, 342.
(52) Atkinson, R.; Aschmann, S. M.; Arey, J. *Environ. Sci. Technol.* **1992**, *26*, 1397.
(53) Olariu, R. I.; Klotz, B.; Barnes, I.; Becker, K. H.; Mocanu, R. *Atmos. Environ.* **2002**, *36*, 3685.
(54) Knispel, R.; Koch, R.; Siese, M.; Zetzsch, C. *Ber. Bunsen-Ges. Phys. Chem.* **1990**, *94*, 1375.
(55) Raghavan, N. V.; Steenken, S. *J. Am. Chem. Soc.* **1980**, *102*, 3495.
(56) Lundqvist, M. J.; Eriksson, L. A. *J. Phys. Chem. B* **2000**, *104*, 848.
(57) Chen, C.-C.; Bozzelli, J. W.; Farrell, J. T. *J. Phys. Chem. A* **2004**, *108*, 4632.
(58) García-Cruz, I.; Castro, M.; Vivier-Bunge, A. *J. Comput. Chem.* **2000**, *21*, 716.
(59) Fan, J.; Zhang, R. *J. Phys. Chem. A* **2006**, *110*, 7728.
(60) Lee, J. E.; Choi, W.; Mhin, B. J.; Balasubramanian, K. *J. Phys. Chem. A* **2004**, *108*, 607.
(61) Atkinson, R. *Phys. Chem. Ref. Data. Monogr.* **1989**, *1*, 1.
(62) Procaccini, C.; Bozzelli, J. W.; Longwell, J. P.; Sarofim, A. F.; Smith, K. A. *Environ. Sci. Technol.* **2003**, *37*, 1684.
(63) Platz, J.; Nielsen, O. J.; Wallington, T. J.; Ball, J. C.; Hurley, M. D.; Straccia, A. M.; Schneider, W. F.; Sehested, J. *J. Phys. Chem. A* **1998**, *102*, 7964.
(64) Fox, T.; Kollman, P. A. *J. Phys. Chem.* **1996**, *100*, 2950.
(65) Francisco, J. *Combust Flame* **1999**, *119*, 312.
(66) Abou-Rachid, H.; Bonneviot, L.; Xu, G.; Kaliaguine, S. *J. Mol. Struct.: THEOCHEM* **2003**, *621*, 293.
(67) Bogdanchikov, G. A.; Baklanov, A. V.; Parker, D. H. *Chem. Phys. Lett.* **2004**, *385*, 486.
(68) Emdee, J. L.; Brezinsky, K.; Glassman, I. *J. Phys. Chem.* **1992**, *96*, 2151.
(69) Oehlschlaeger, M. A.; Davidson, D. F.; Hanson, R. K. *Combust. Flame* **2006**, *147*, 195.